

ADA078007

RADC-TR-79-235
Interim Report
September 1979

PRO 6296P
12

LEVEL ~~12~~



HIGH POWER MILLIMETER WAVE AMPLIFIER

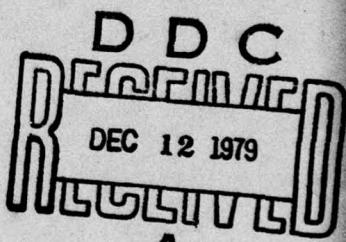
Varian Associates, Inc.

Sponsored by
Defense Advanced Research Projects Agency (DoD)
ARPA Order No. 3192

and

Ballistic Missile Defense
Advanced Technology Center (Army)

APPROVED FOR PUBLIC RELEASE; DISTRIBUTION UNLIMITED



DDC FILE COPY

The views and conclusions contained in this document are those of the authors and should not be interpreted as necessarily representing the official policies, either expressed or implied, of the Defense Advanced Research Projects Agency or the U. S. Government.

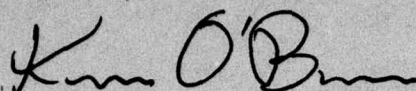
**ROME AIR DEVELOPMENT CENTER
Air Force Systems Command
Griffiss Air Force Base, New York 13441**

79 12 11 003

This report has been reviewed by the RADC Information Office (OI) and is releasable to the National Technical Information Service (NTIS). At NTIS it will be releasable to the general public, including foreign nations.

RADC-TR-79-235 has been reviewed and is approved for publication.

APPROVED:



KEVIN O'BRIEN, 1Lt, USAF
Project Engineer

If your address has changed or if you wish to be removed from the RADC mailing list, or if the addressee is no longer employed by your organization, please notify RADC (OCTP), Griffiss AFB NY 13441. This will assist us in maintaining a current mailing list.

Do not return this copy. Retain or destroy.

HIGH POWER MILLIMETER WAVE AMPLIFIER

S. Hegji
H. Jory
R. Morwood
A. Nordquist
R. Symons

Contractor: Varian Associates, Inc.
Contract Number: F30602-78-C-0011
Effective Date of Contract: 31 October 1977
Contract Expiration Date: 1 November 1979
Short Title of Work: High Power Millimeter Wave Amp
Program Code Number: 7E20
Period of Work Covered: Nov 78 - Apr 79

Principal Investigator: Howard Jory
Phone: 415 493-4000

Project Engineer: 1Lt Kevin O'Brien
Phone: 315 330-4381

Approved for public release; distribution unlimited.

This research was supported by the Defense Advanced Research Projects Agency of the Department of Defense and was monitored by 1Lt Kevin O'Brien (OCTP), Griffiss AFB NY 13441 under Contract F30602-78-C-0011.

Accession For	
NTIS GRADE	
DDC TAB	
Unannounced	
Justification	
By	
Distribution	
Availability Codes	
Distr	Available/or special

79 12 11 003

UNCLASSIFIED

SECURITY CLASSIFICATION: 1 OF THIS PAGE (When Data Entered)

DD FORM 1 JAN 73 1473

UNCLASSIFIED

SECURITY CLASSIFICATION OF THIS PAGE (When Data Entered)

406 552

LB

UNCLASSIFIED

SECURITY CLASSIFICATION OF THIS PAGE(When Data Entered)

Also included in this report are further calculations on TE Gyro-TWT's operating in the fundamental and the second harmonic using a small signal dispersion relation computer program.

UNCLASSIFIED

SECURITY CLASSIFICATION OF THIS PAGE(When Data Entered)

TABLE OF CONTENTS

<u>Section</u>		<u>Page</u>
I.	INTRODUCTION	1
II.	HISTORY OF THE PHASE I AMPLIFIER: VGX-8080 S/N 1	3
III.	HISTORY OF THE GYRO-TWT: VGC-8160 S/N 1 AND 1R	7
IV.	TEST OF THE GYRO-TWT: 1ST REBUILD	10
V.	SECOND REBUILD OF THE GYRO-TWT: VGC-8160 S/N 1R2	16
VI.	THEORY AND COMPUTATIONS	19
VII.	CONCLUSIONS AND PLANS	25

LIST OF ILLUSTRATIONS

<u>Figure</u>		<u>Page</u>
1.	Field Profile of Longer Solenoid used for VGC-8160 S/N 1R....	11
2.	Gain vs Frequency for VGC-8160 S/N 1R1	12
3.	Gain vs Beam Current for VGC-8160 S/N 1R1	13
4.	Output with Beam vs Output Without Beam VGC-8160 S/N 1R	15
5.	VGC-8160 Reflected Power Input Transition	17
6.	Input Match (Reflected Power) for VGC-8160 S/N 1 RF Circuit Only (Paper Load)	18
7.	Gyro-TWT Dispersion Relation for $\Omega_0/\omega_c = 1.05 P/P = 1$	20
8.	Gyro-TWT Dispersion Relation for $\Omega_0/\omega_c = 1.05 P/P = 2$	22
9.	Gyro-TWT Dispersion Relation for $\Omega_0/\omega_c = 0.54 P/P = 2$	22
10.	Gyro-TWT Dispersion Relation for $\Omega_0/\omega_c = 0.55 P/P = 2$	23
11.	Gyro-TWT Dispersion Relation for $\Omega_0/\omega_c = 0.56 P/P = 2$	24

I. INTRODUCTION

The objective of this program is to design a high power pulsed amplifier for millimeter wave operation. Desired operating characteristics are:

center frequency	94 GHz
electronic bandwidth	> 4%
peak power	100 kW
average power	10 kW
beam efficiency	30%
power gain	30 dB

The development is limited to the consideration of gyrotron-type amplifiers which involve an interaction based on cyclotron resonance.

The present program was preceded by a Phase I study effort⁽¹⁾ which explored the feasibility of gyrokylystron amplifiers with cyclotron harmonic operation. As part of the study effort, a three-cavity gyrokylystron amplifier operating on the second harmonic of the cyclotron frequency at X-band was built and partially tested.

The first interim report for Phase II⁽²⁾ covered the completion of testing of the X-band gyrokylystron built under the previous study program. Measurements of saturated output power were included in the report. Spectrum measurements and noise figure measurements were also presented.

In addition, the report contained a discussion of the alternatives which were considered for converting the three-cavity gyrokylystron to the gyro-TWT.

The second Phase II interim report⁽³⁾ describes results on the first TE₁₁⁰ mode gyro-TWT experiment which demonstrated some net gain. The gain figures were somewhat lower than expected, perhaps due to large launching losses. Also described in Section VI of that report are results of a small signal gain program which seem to indicate the possibility of mode competition in gyro-TWTs using modes higher than the lowest waveguide mode.

The possibility of wider bandwidth and higher gain per unit length gyro-TWTs using periodic circuits (which slow the wave slightly, concentrate the electric field in the region of the beam, and hence increase the circuit impedance) were investigated. The results are described in Section VIII of the second interim report. However, the difficulty of building such circuits for 94 GHz operation and the encouraging performance of the second TE₁₁ gyro TWT experiment, described in this report, have led us to suspend further work on this approach.

The adaptation of the NRL CYLMAS large signal program to the Varian computer has been successful and was described in Section VII of the second interim report. Additional changes which lead to more economical use of computer memory are described in this report. The BASIC small signal program described in Section VI of the second interim report has been modified to calculate the gain of azimuthally-varying, circularly-polarized, TE mode gyro TWT's such as our TE₁₁ experimental tube.

II. HISTORY OF THE PHASE I AMPLIFIER: VGX-8080 S/N 1

The amplifier constructed in Phase I was a three-cavity gyrokylystron, for operation at 10.35 GHz. It was designed to operate at the second harmonic of the cyclotron resonance. The resonance condition is given by the equation

$$\omega = \frac{neB}{\gamma m_0} \quad (1)$$

where ω is the operating frequency, B is the axial dc magnetic field, e/m_0 is the charge-to-mass ratio of the electron, γ is the relativistic mass factor, and n is the harmonic number. Operation at the second harmonic of the resonance allows the magnetic field to be smaller by a factor of two.

The operating parameters for the 10.35 GHz amplifier are given in Table I. Additional information on the design is included in the final report for Phase I⁽¹⁾.

Initial operation resulted in the observation of a microwave gain of 9 to 10 dB under small signal conditions where the power output was about 100 w peak. This operation was achieved at reduced beam voltage of 40 kV. Amplifier operation at higher beam voltage had been prevented by interfering oscillations involving the TE₁₁₁ resonance in the input cavity interacting with the fundamental cyclotron resonance condition. The oscillation occurred at a frequency near 5.4 GHz and was somewhat tunable depending on main magnetic field values. Table 2 shows a summary of preliminary test values compared to design values.

At the start of Phase II, a linear-beam klystron capable of about 8 kw peak output power was installed as a driver for the gyrokylystron, allowing the gyrokylystron to be driven to saturation. The highest values of saturated power, small signal gain, and efficiency are listed in Table 3. Curves relating the tube performance to the available parameters, beam voltage and current, anode voltage, and magnetic field, can be found in the first interim report.⁽²⁾

TABLE 1
10.35 GHz AMPLIFIER DESIGN VALUES

1. Power output - peak	100	kw
average	5	kW
2. Gain	30	dB
3. Bandwidth	0.1	%
4. Magnetic field	1.96	kg
5. RF circuits (TE_{011} cavities)		
Input cavity length	1.5	λ *
First drift length	1.2	λ
Center cavity length	1.5	λ
Second drift length	1.2	λ
Output cavity length	3	λ
Cavity loaded Q (each cavity)	1000	
Drift tube radius (0.51)	0.58	in
6. Beam		
Voltage	60	kV
Current	5	A
Outer beam radius	0.53	in
Inner beam radius	0.19	in
Axial velocity	0.2	c **
Transverse velocity	0.4	c
Electron orbit radius	0.15	in

* λ = Free-space wavelength at the operating frequency

** c = velocity of light

TABLE 2
SUMMARY OF PRELIMINARY TEST RESULTS

<u>Parameter</u>	<u>Design Value</u>	<u>Preliminary Test Value</u>
Beam voltage	60 kV	40 kV
Gun anode voltage	31 kV (52%)	24 kV (60%)
Beam current	5 A	4.5 A
Main magnet field	1960 g	1960 g \pm 5%
Gun magnet	485 g	450 g \pm 10%
Microwave gain	23-26 dB	9-10 dB
Peak body current	0	80 ma
Peak gun anode current	0	<4 ma

TABLE 3
BEST PERFORMANCE

<u>Parameters</u>	<u>Test Value</u>
Beam voltage	50 kV
Beam current	5.0 A
Saturated power	20.56 kW
Small signal gain	5.8 dB
Gain compression	1.4 dB
Saturated efficiency	8.2%

III. HISTORY OF THE GYRO-TWT: VGC-8160 S/N 1 and 1R

The gyro-TWT version of the family of cyclotron resonance masers differs from the klystron or monotron by virtue of its non-resonant rf circuit. The beam is well-coupled to the EM fields over a reasonable bandwidth (5-10%). Unlike a conventional (linear beam) TWT, the gyro-TWT utilizes a fast-wave interaction between circuit and beam. This allows the use of simple, non-periodic rf circuits.

The initial gyro-TWT experiment was designed to employ the TE_{11} mode in a circular guide and to operate at the fundamental cyclotron resonance, about 5.2 GHz. The input coupling system had to fit within the magnet bore, which was difficult at 5.2 GHz with conventional rectangular waveguide components. An attempt was made to couple to the rf circuit using a coaxial transmission line terminated in a probe or loop. The close proximity of the beam to the wall of the interaction circuit required the use of small loops or probes which had high radiation resistances, and required excessive impedance transformation to achieve an acceptable match. A hybrid solution was found involving coupling to the circuit with a rectangular waveguide port and then using a vacuum tight coax-to-waveguide transition. The matching for the rectangular guide to the interaction circuit required a capacitance at the junction. Since two orthogonal TE_{11} modes can exist, two inputs were required separated 90° azimuthally.

Since the gyro-TWT experiment utilized a different circuit mode, a change in the output window design was required. The previous window design had an axial break in the guide wall suitable for the TE_{01} mode and was matched for operation at 10.35 GHz. For use with TE_{11} mode, the axial wall gap had to be removed, and the window thickness increased to obtain a C-band match. Transmission measurements on the window revealed several trapped window modes above the band, with the lowest at the upper band edge.

Table IV shows the design values for the gyro-TWT. The rf circuit length was determined primarily by the size of the available magnet. The test results for the first gyro-TWT experiment are discussed in detail in Section IV of the

second interim report⁽³⁾. To summarize: oscillations in several modes and frequencies were observed (see Figure 1). Amplification in the 0-3 dB range was obtained, but was insufficient for good measurements. During the test, improved small-signal calculations indicated that the expected gain was of the same order as the launching losses. On the basis of these results, a rebuild was performed which incorporated an extra length of interaction circuit, calculated to yield 20 dB more gain. A larger magnet was obtained to accommodate this change.

TABLE 4

5.2 GHz GYRO-TWT DESIGN VALUES

1. Power Output - peak	~ 100	kW
- average	~ 5	kW
2. Gain	~ 20-30	dB
3. Bandwidth	5.0	%
4. Magnetic field	1.96	kG
5. RF Circuit (circular waveguide)		
Guide length	5.1	λ^*
Guide radius	0.72	in
6. Beam		
Voltage	60	kV
Current	5	A
Outer beam radius	0.53	in
Inner beam radius	0.19	in
Axial velocity	0.2	c^{**}
Transverse velocity	0.4	c
Electron orbit radius	0.15	in

* λ = Free-space wavelength at the operating frequency.

** c = velocity of light (in vacuum).

IV. TEST OF THE GYRO-TWT: 1ST REBUILD

Initial tests with the gyro-TWT rebuild, VGC-8160 S/N-1R, indicated poor beam transmission. The tube was removed from the socket and the axial magnetic field profile of the new, longer solenoid was investigated. The measurements indicated insufficient field at the cathode position, so an additional coil was added to the assembly. Figure 1 shows the actual field profile achieved along with the profile used in the gun design simulations.

After verifying good beam transmission in the adjusted magnetic circuit, the tube was brought up to full operating parameters. The first rf output observed were oscillations occurring in the same two frequency ranges which had been observed in the original build⁽³⁾. Specifically, the oscillations were confined to the 4.9 and 8.1 GHz regions, and were calorimetrically measured to have peak output powers of 45 kW and 14 kW respectively at a beam power of 300 kW.

When the beam's transverse energy was slightly reduced by increasing the cathode magnetic field, the onset of oscillation was discouraged and amplification was observed. Small-signal measurements yielded a maximum of 17 dB gain at 4.9 GHz, with a beam voltage of 45 kV, and a beam current of 2.5 A. The low values of voltage and current tended to yield higher possible gain values. The lower total beam power allowed setting the gun magnets for higher transverse energy without the occurrence of oscillations.

Figure 2 shows the variation in small-signal gain at various frequency points over the band of detectable amplification. It is felt that the large variations in gain are associated with the poor tube match (input and output) between 4.9 and 5.1 GHz. At the higher frequencies, 5.1 to 5.3 GHz, the match is better, the interaction is weaker, and the magnetic field may not be optimized, in order to avoid oscillation.

The dependence of gain on beam current was investigated and is shown in Figure 3. This measurement was also made at more stable values of beam transverse energy.

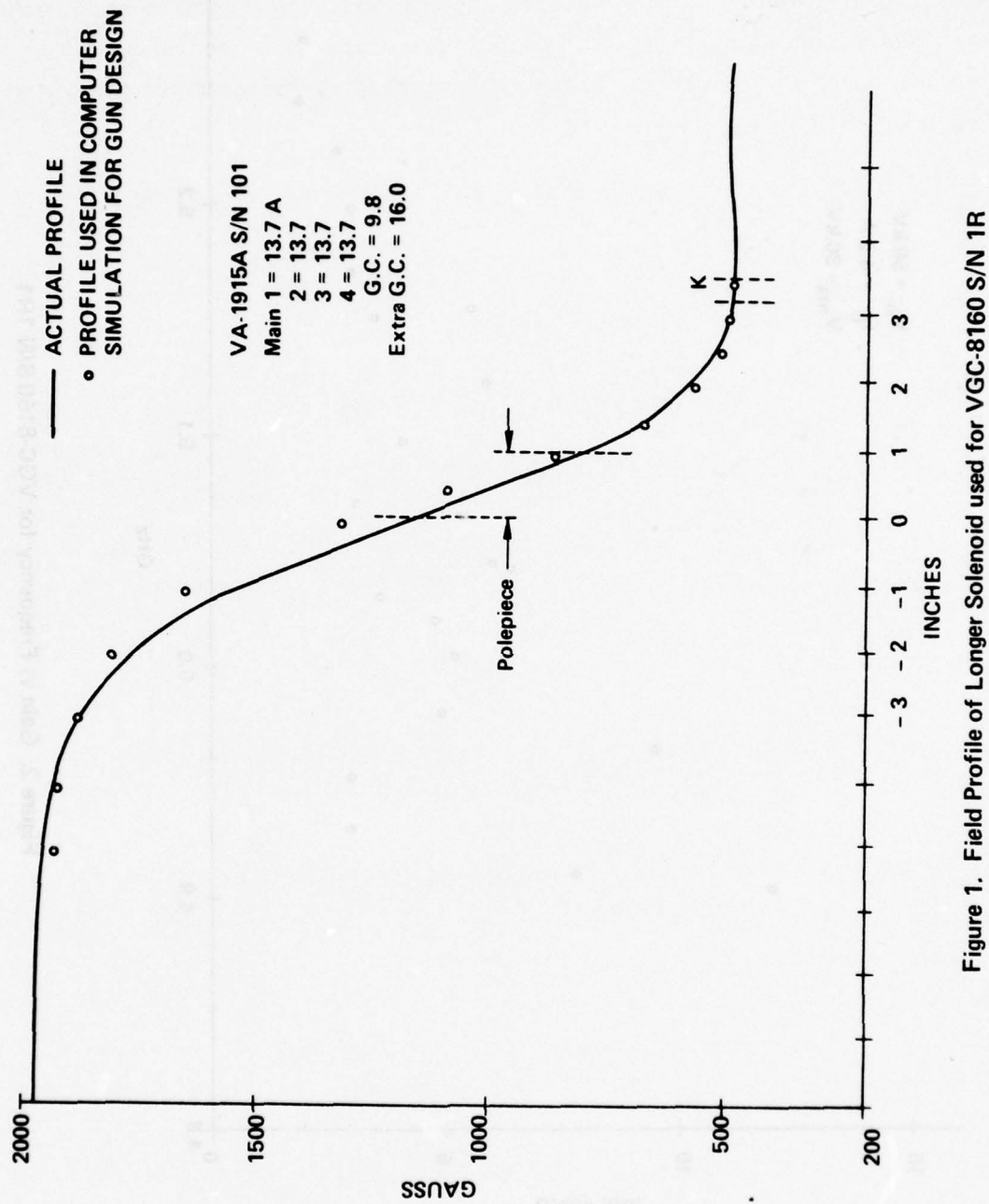


Figure 1. Field Profile of Longer Solenoid used for VGC-8160 S/N 1R

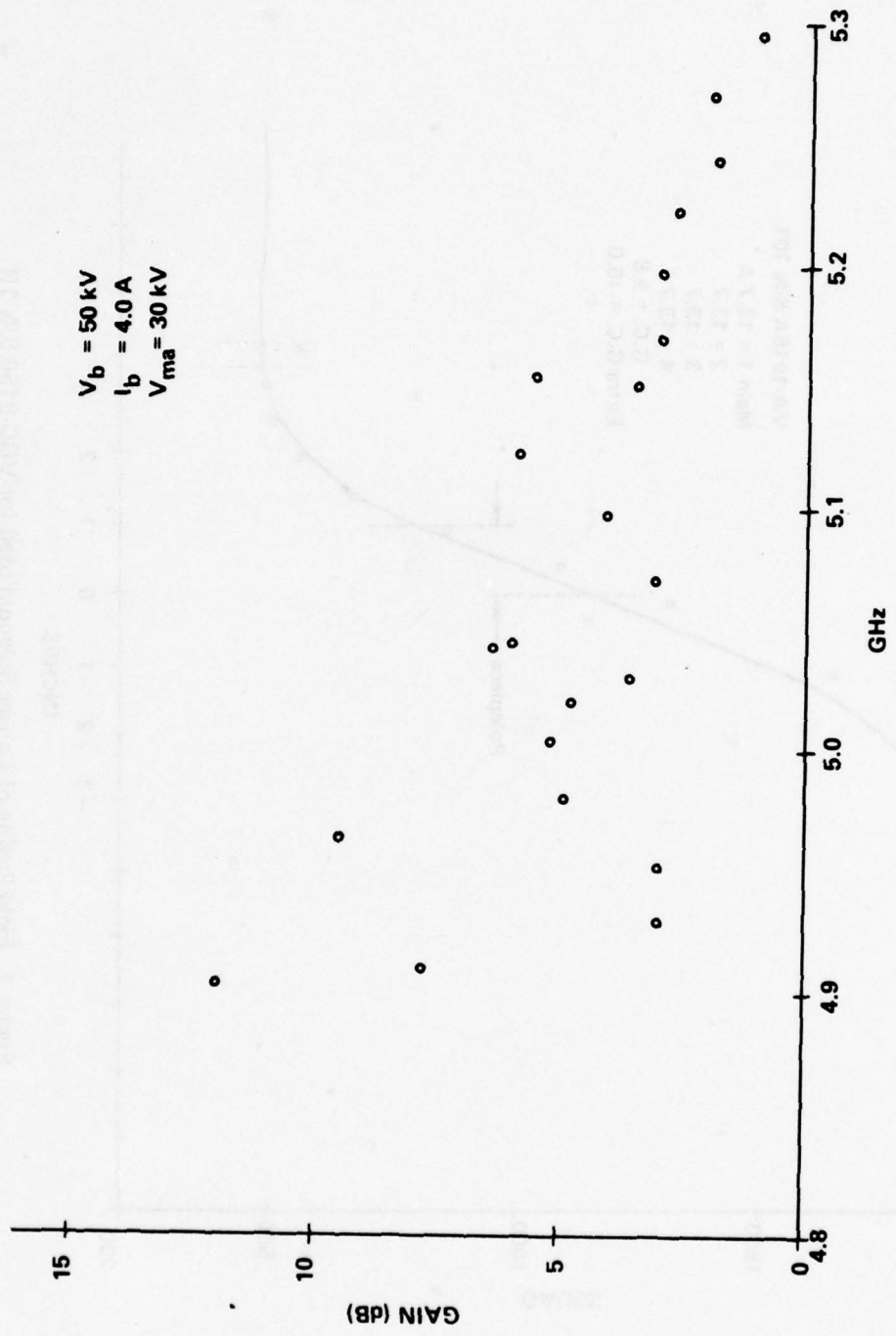


Figure 2. Gain vs Frequency for VGC-8160 S/N 1R1

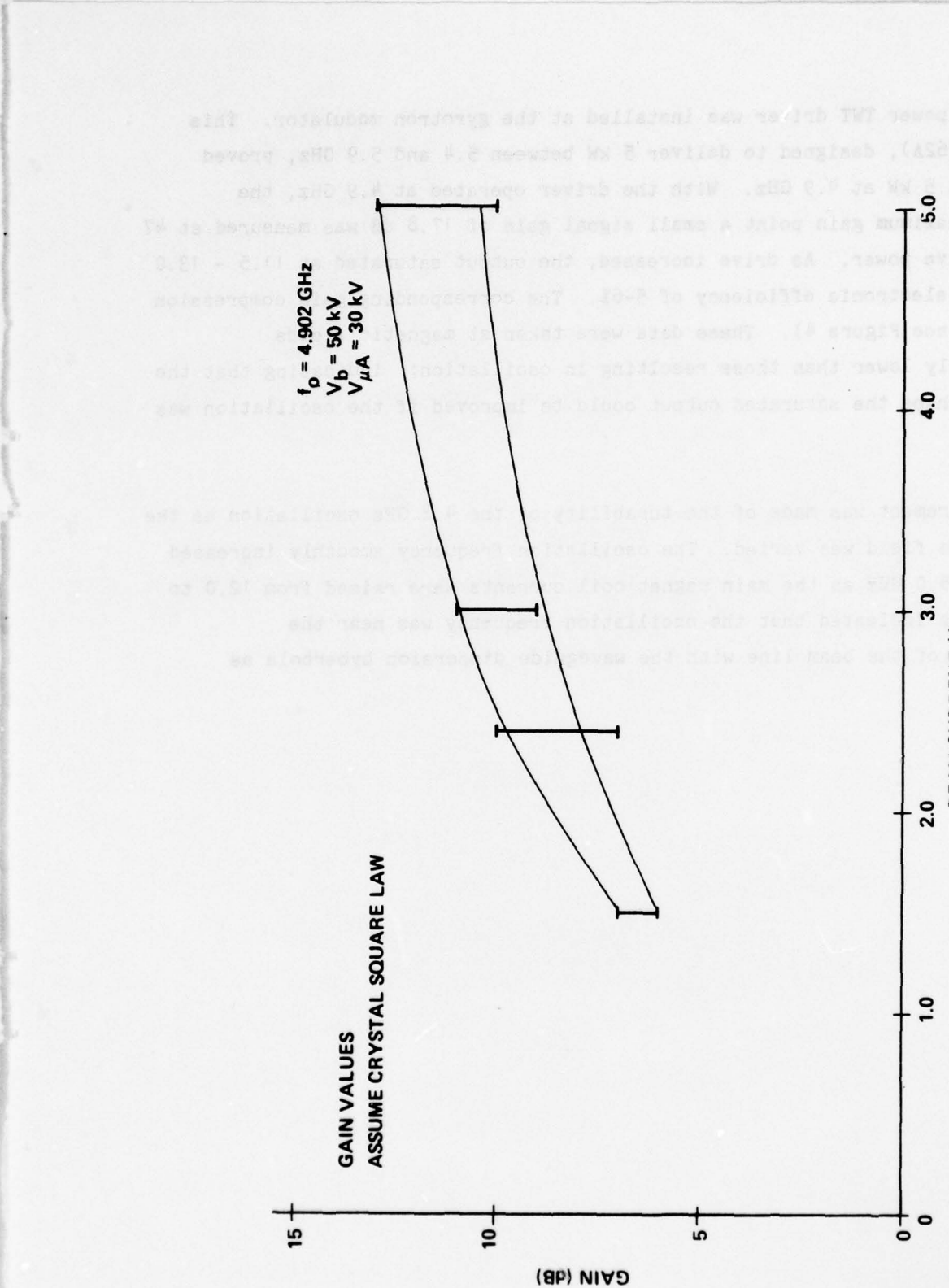


Figure 3. Gain vs Beam Current for VGC-8160 S/N 1R1

A high power TWT driver was installed at the gyrotron modulator. This tube (VTC-5262A), designed to deliver 5 kW between 5.4 and 5.9 GHz, proved capable of 2.5 kW at 4.9 GHz. With the driver operated at 4.9 GHz, the gyrotron's maximum gain point a small signal gain of 17.8 dB was measured at 47 watts of drive power. As drive increased, the output saturated at 11.5 - 13.0 kW, with an electronic efficiency of 5-6%. The corresponding gain compression was 3.0 dB (see Figure 4). These data were taken at magnetic fields differentially lower than those resulting in oscillation; indicating that the gain and perhaps the saturated output could be improved if the oscillation was stabilized.

A measurement was made of the tunability of the 4.8 GHz oscillation as the main magnetic field was varied. The oscillation frequency smoothly increased from 4.8 to 5.0 GHz as the main magnet coil currents were raised from 12.0 to 15.0 A. This indicated that the oscillation frequency was near the intersection of the beam line with the waveguide dispersion hyperbola as expected.

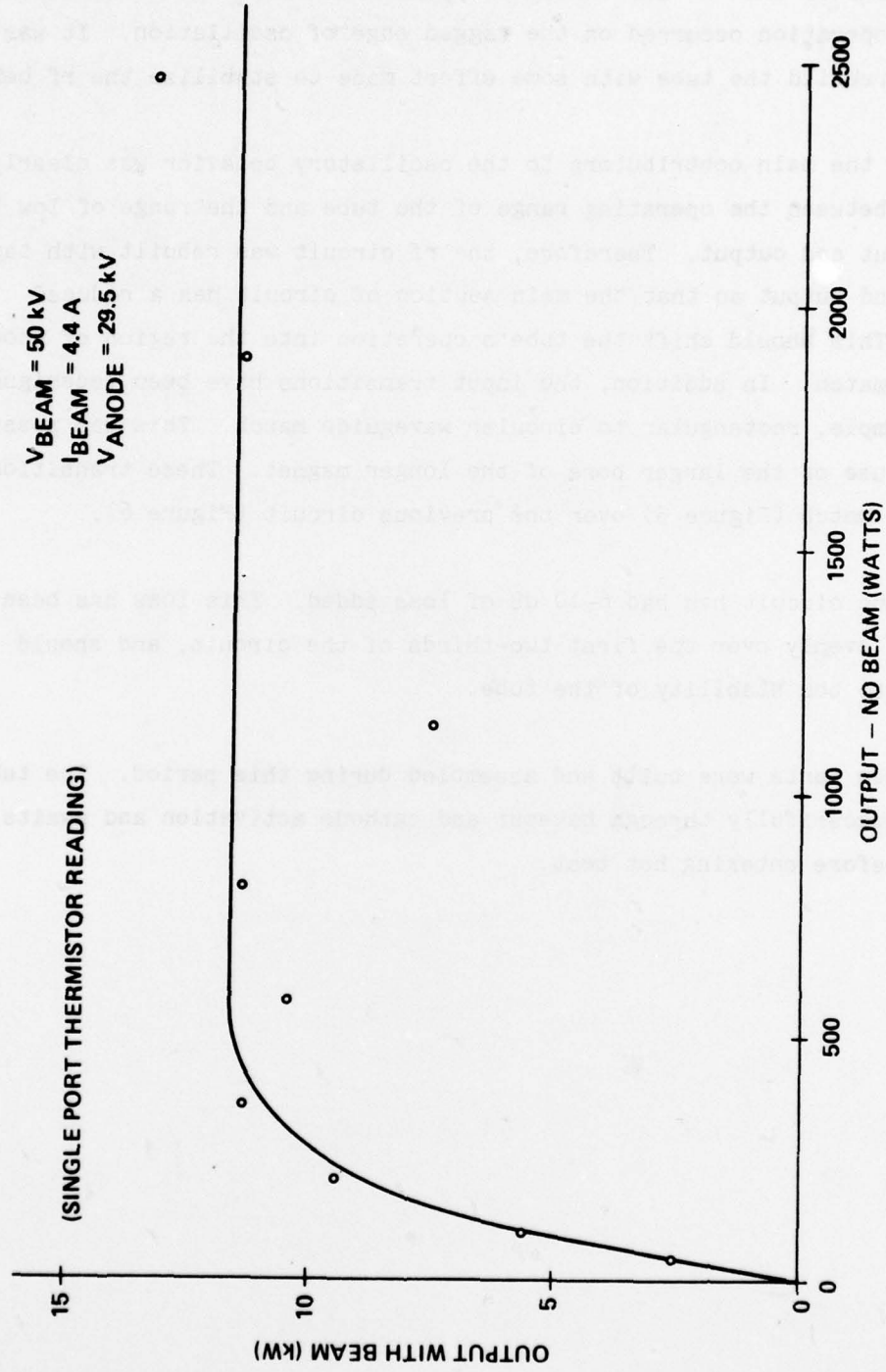


Figure 4. Output with Beam vs Output Without Beam VGC-8160 S/N 1R

V. SECOND REBUILD OF THE GYRO-TWT: VGC-8160 S/N 1R2

The VGC-8160 S/N 1R1 was touchy to operate since the most interesting regions of operation occurred on the ragged edge of oscillation. It was decided to rebuild the tube with some effort made to stabilize the rf behavior.

One of the main contributors to the oscillatory behavior was clearly the difference between the operating range of the tube and the range of low VSWR for the input and output. Therefore, the rf circuit was rebuilt with tapers at the input and output so that the main section of circuit has a reduced diameter. This should shift the tube's operation into the region of good input and output match. In addition, the input transitions have been redesigned around a simple, rectangular to circular waveguide match. This was possible due to the use of the larger bore of the longer magnet. These transitions have an improved match (Figure 5) over the previous circuit (Figure 6).

Also the circuit has had 6-10 dB of loss added. This loss has been distributed evenly over the first two-thirds of the circuit, and should contribute to the stability of the tube.

The tube parts were built and assembled during this period. The tube processed successfully through bakeout and cathode activation and awaits final cold test before entering hot test.

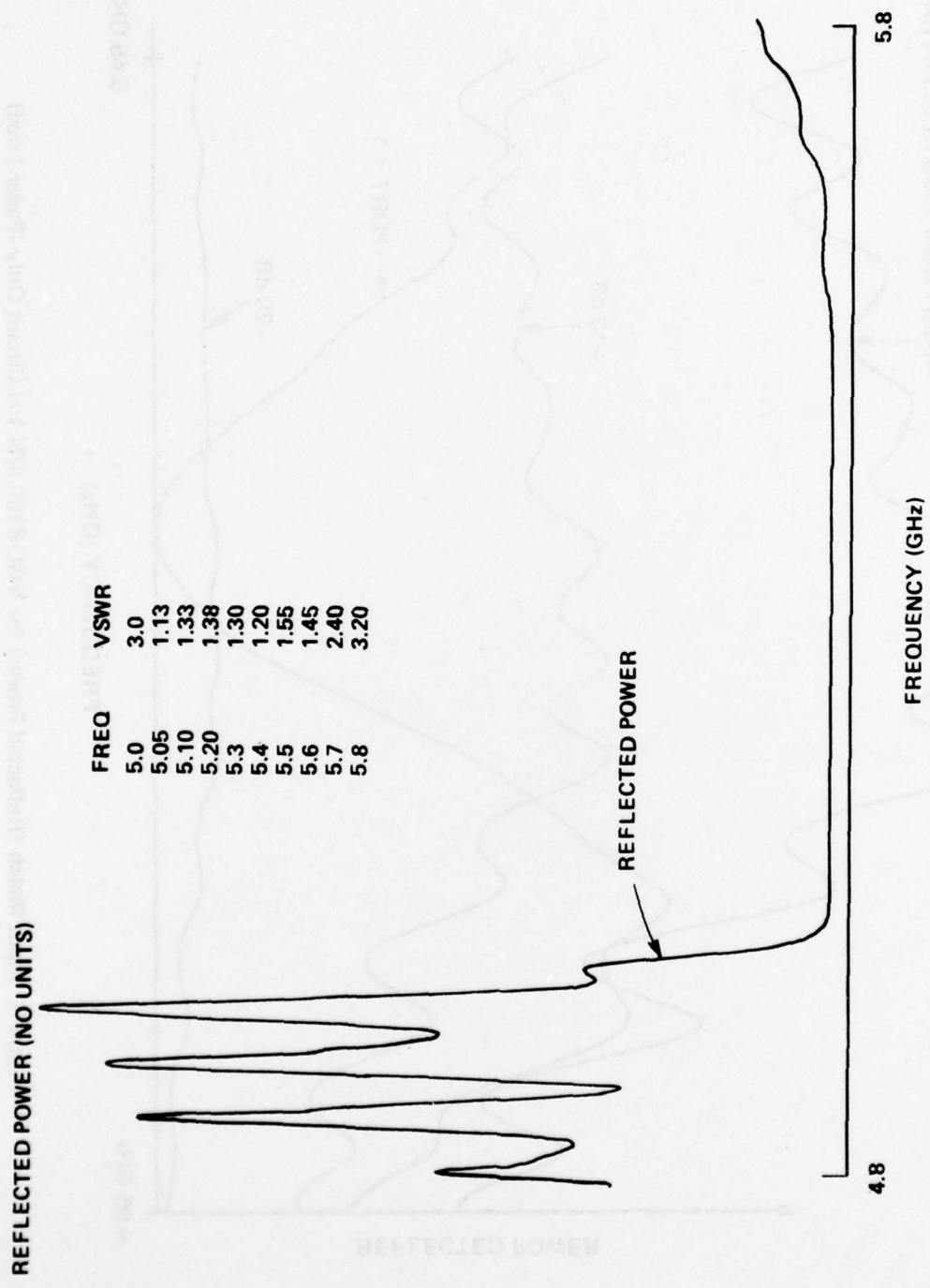


Figure 5. VGC-8160 Reflected Power Input Transition

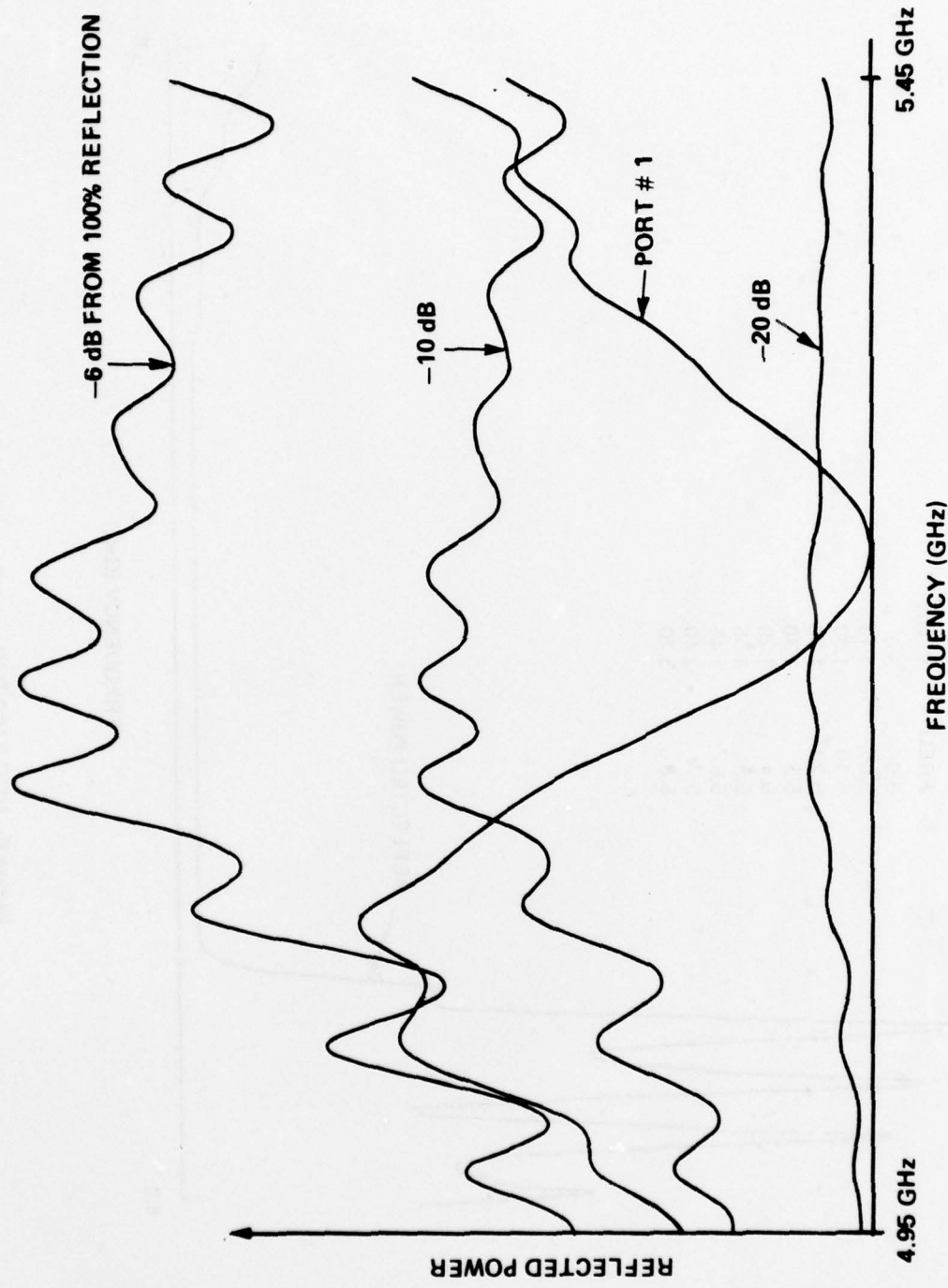


Figure 6. Input Match (Reflected Power) for VGC-8160 S/N 1 rf Circuit Only (Paper Load)

VI. THEORY AND COMPUTATIONS

Since the last interim report, use of core memory for the CYLMAS program has been reduced by storing the information in the output data matrices on disc. This permits the use of a larger number of particles in order to handle more complex beam distributions in either position or velocity space.

The small signal BASIC gyro-TWT dispersion relation program has been modified to permit calculations for azimuthally varying, circular-polarized, TE modes as described by Chu⁽⁴⁾ et al. In addition, the program has been changed so that the spatial growth rate is calculated automatically by dividing the temporal growth by the group velocity for each value of k .

A series of dispersion diagrams are shown in Figures 7 through 11 for both fundamental and second cyclotron harmonic operation of all our TE₁₁ gyro-TWTs. These diagrams give values of $\omega = \omega_r + j\omega_i$ as a function of k for the wave $H_z(z,t) = H_{z0} e^{j(\omega_r t - k_z z)} + \omega_i t$ in which H_z is the z component of magnetization in the waveguide, H_{z0} is its value at $z = 0$, k is the phase constant or wavenumber, ω_r is the real part of the frequency and ω_i is the imaginary part of frequency or temporal growth rate. The spatial growth rate may be found by the relation $k_i = \omega_i \left(\frac{\partial \omega_r}{\partial k} \right)^{-1}$ when it is desired to express the wave as $H_z(z,t) = H_{z0} e^{j(\omega_r - k_z) t + k_i z}$.

Figure 7 is for fundamental operation with the ratio of perpendicular to parallel momentum (p_\perp/p_\parallel) equal to one. Figures 8 through 11 are curves for a ratio of two with magnetic field as the parameter. It can be seen that the growth rate for second cyclotron harmonic operation is about one-half that for fundamental interaction. In the curves the ordinate is normalized to the waveguide cutoff frequency ω_c and the abscissa is normalized to $k_c = \omega_c/c$.

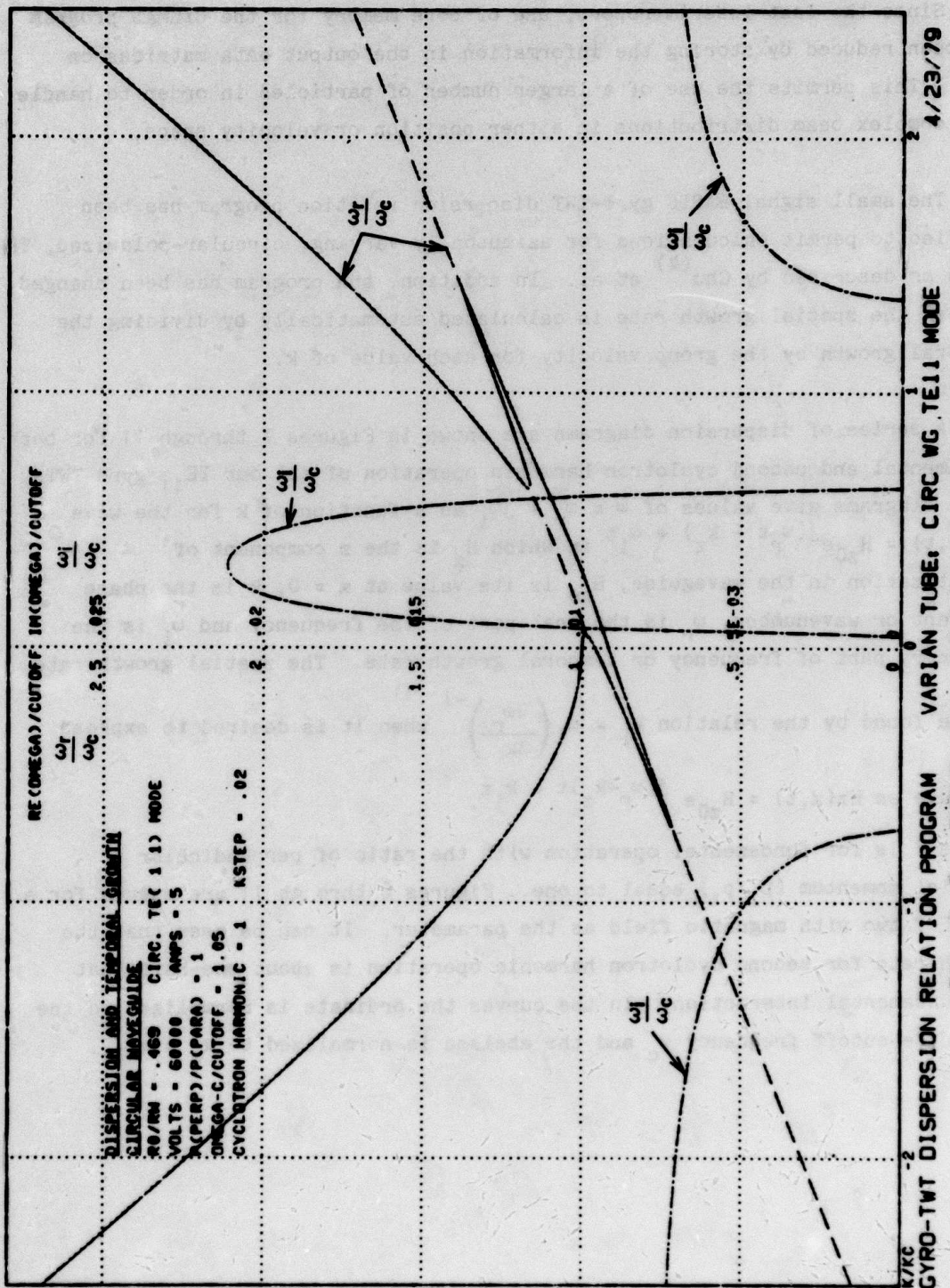


Figure 7. Gyro-TWT Dispersion Relation for $\Omega_0/\omega_c = 1.05$ $P_T/P_{\parallel} = 1$

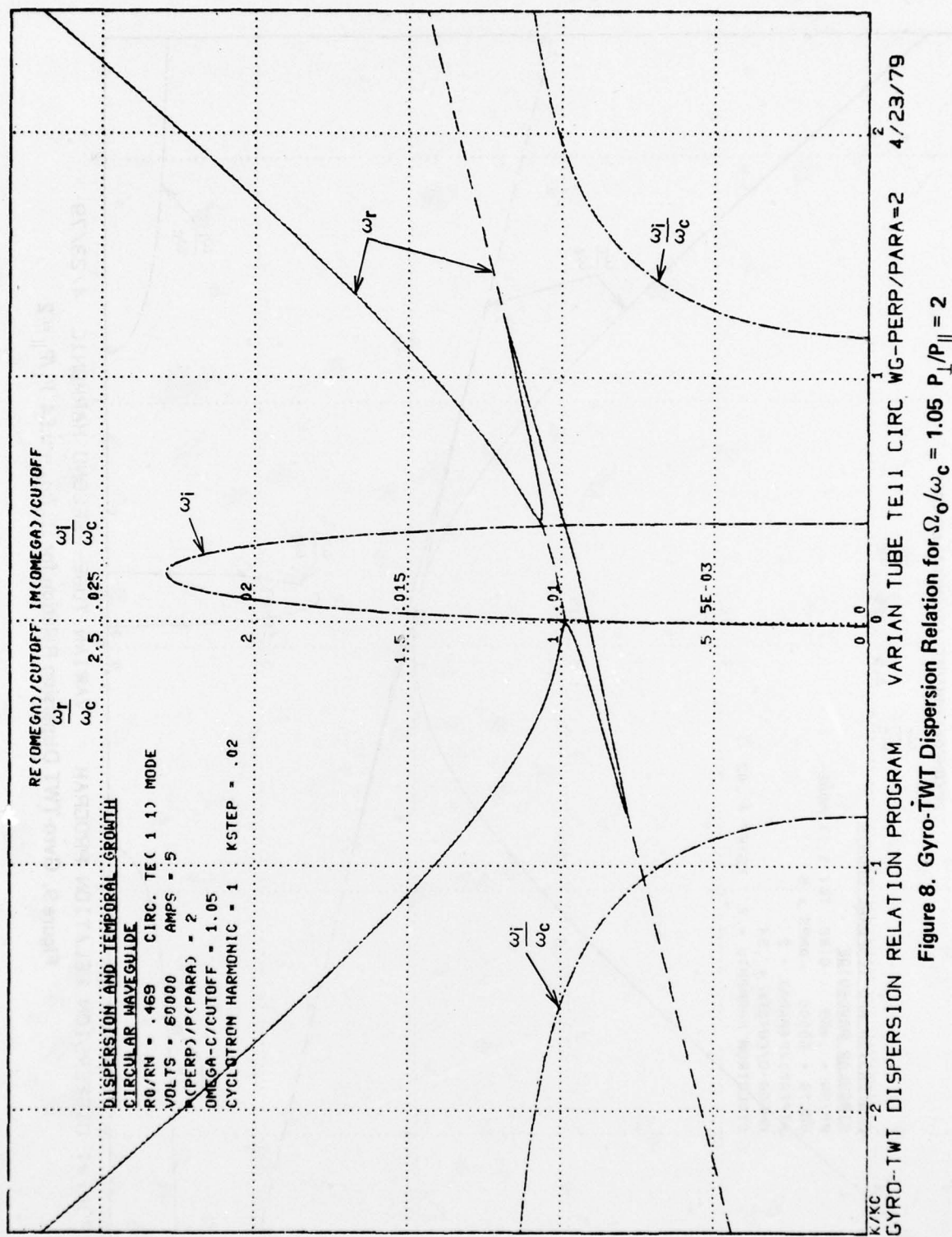


Figure 8. Gyro-TWT Dispersion Relation for $\Omega_0/\omega_c = 1.05$ $P_{\perp}/P_{\parallel} = 2$

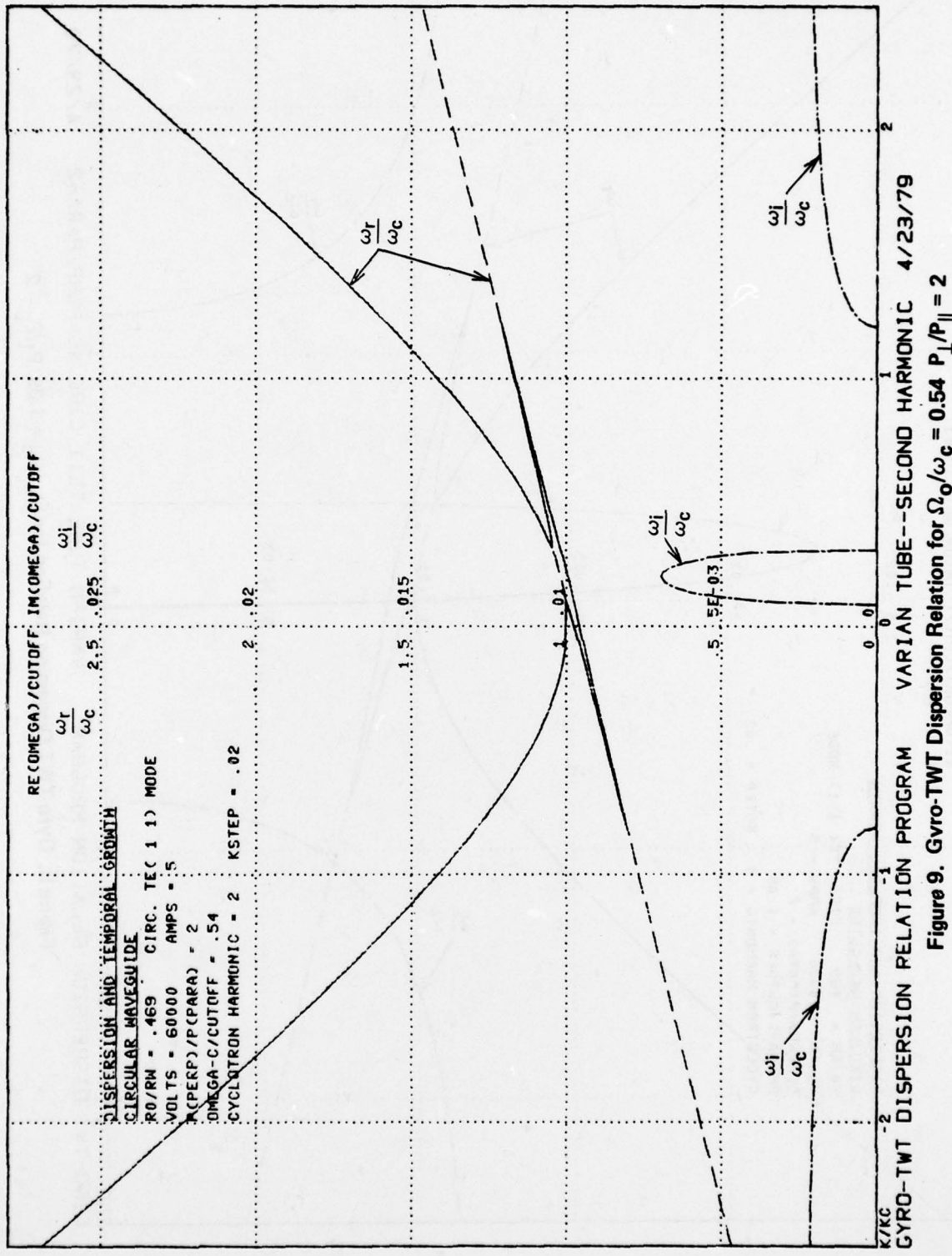
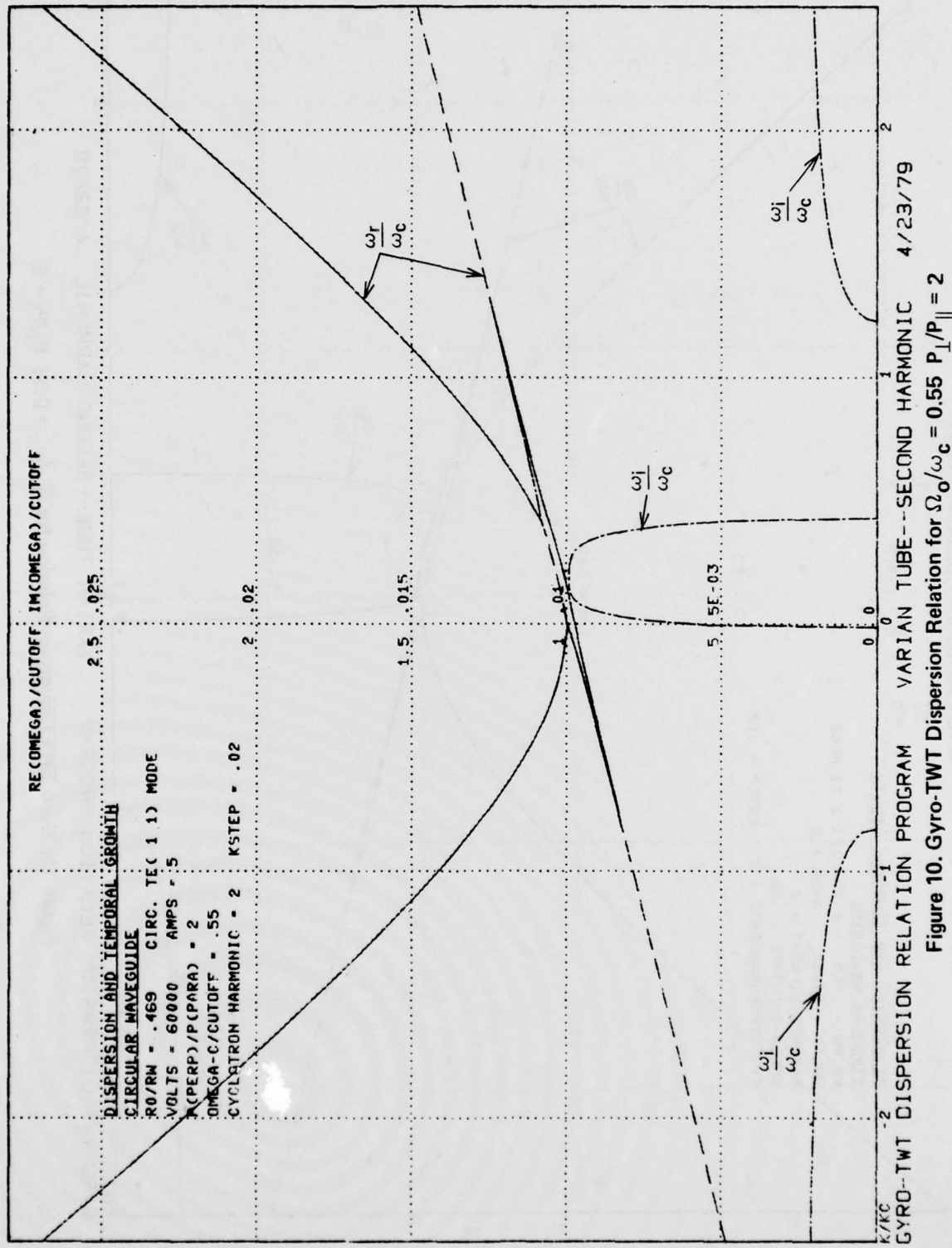


Figure 9. Gyro-TWT Dispersion Relation for $\Omega_0/\omega_c = 0.54$ $P_{\perp}/P_{\parallel} = 2$ 4/23/79



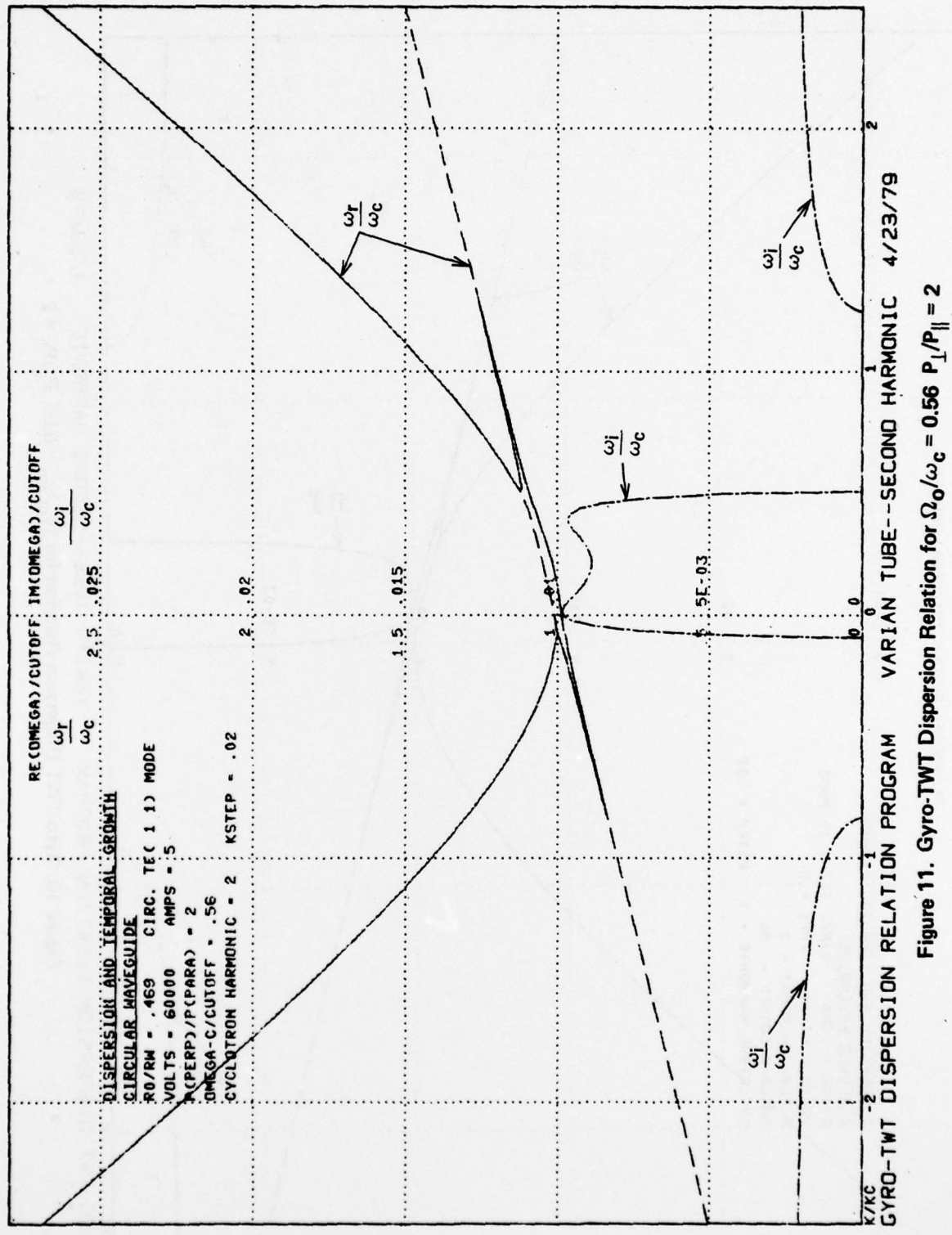


Figure 11. Gyro-TWT Dispersion Relation for $\Omega_0/\omega_c = 0.56$ $P_{\perp}/P_{||} = 2$

VII. CONCLUSIONS AND PLANS

The encouraging performance of the second gyro-TWT experiment leads us to believe that the third experiment, which includes distributed loss and better matches, will probably give results which are adequate to justify the scaling of this design to 94 GHz.

At the moment, testing of the third experimental tube is being delayed by an auto-transformer failure in the test equipment. Not only is every effort being made to repair this piece of test equipment, but we are also pursuing the possibility of testing in another piece of equipment.

As soon as we have data on the third experiment we intend to commence scaling the design to 94 GHz.

REFERENCES

1. Millimeter Wave Gyrotron Development, Phase I Final Technical Report. RADC-TR-77-210, June 1977. Contract F30602-76-C-0237. (A041596)
2. High Power Millimeter Wave Amplifier Interim Report No. 1, Nov. 1, 1977 - March 31, 1978, RADC Contract No. F30602-78-C-0011. RADC TR 78-235 (A062966)
3. High Power Millimeter Wave Amplifier Interim Report No. 2, March 31, 1978 - November 1, 1978, RADC Contract No. F30602-78-C-0011. RADC TR 79-45 (A068915)
4. K.R. Chu, A.T. Drobot, H.H. Szu and P. Sprangle "Analytic Scaling of Efficiency for the Gyrotron Traveling Wave Amplifier Operating at Cyclotron Harmonics", NRL Memorandum Report 3892.

MISSION
of
Rome Air Development Center

RADC plans and executes research, development, test and selected acquisition programs in support of Command, Control Communications and Intelligence (C³I) activities. Technical and engineering support within areas of technical competence is provided to ESD Program Offices (POs) and other ESD elements. The principal technical mission areas are communications, electromagnetic guidance and control, surveillance of ground and aerospace objects, intelligence data collection and handling, information system technology, ionospheric propagation, solid state sciences, microwave physics and electronic reliability, maintainability and compatibility.